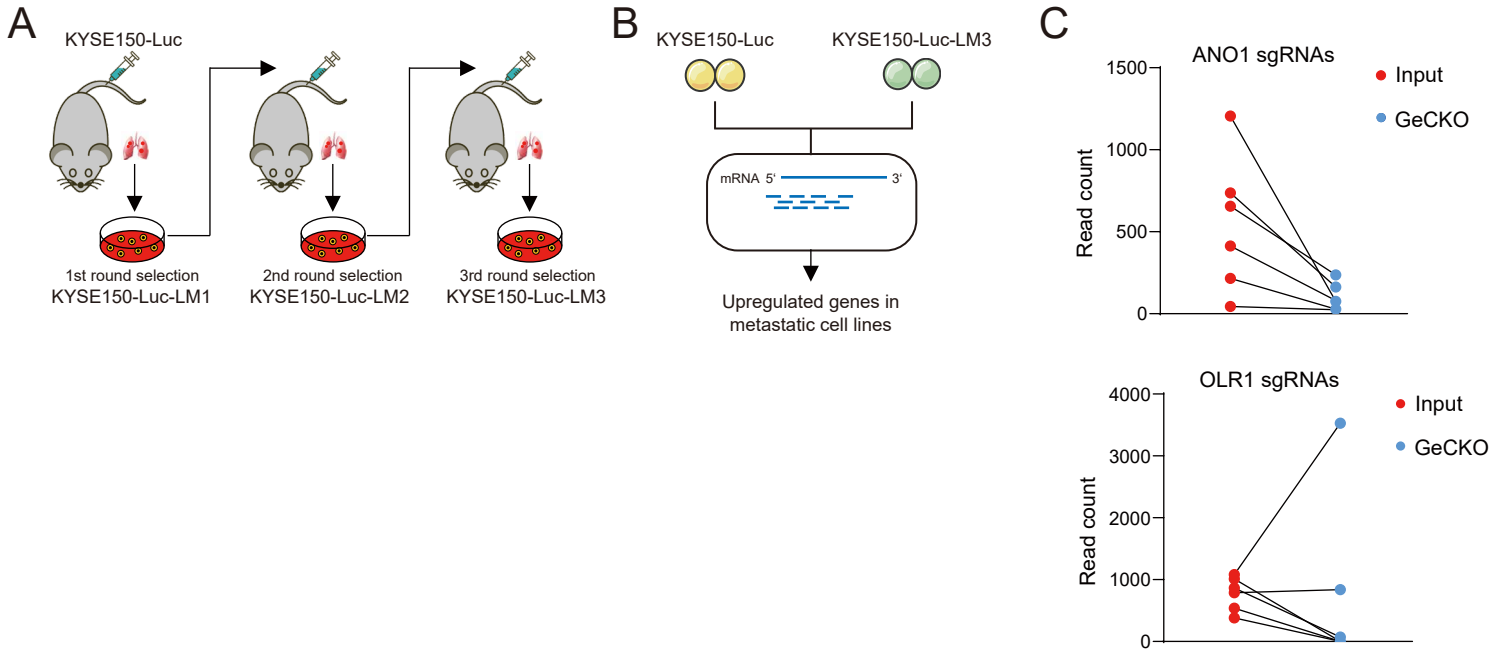

Supplementary Figure 1. (A) Diagram showing the approach to establish the metastatic ESCC cell sublines. **(B)** Our strategy to identify the potential drivers of cancer metastasis. **(C)** Read counts of sgRNAs targeting ANO1 or OLR1 in GeCKO-transduced cells and input cells in a CRISPR/Cas9-based functional screen.

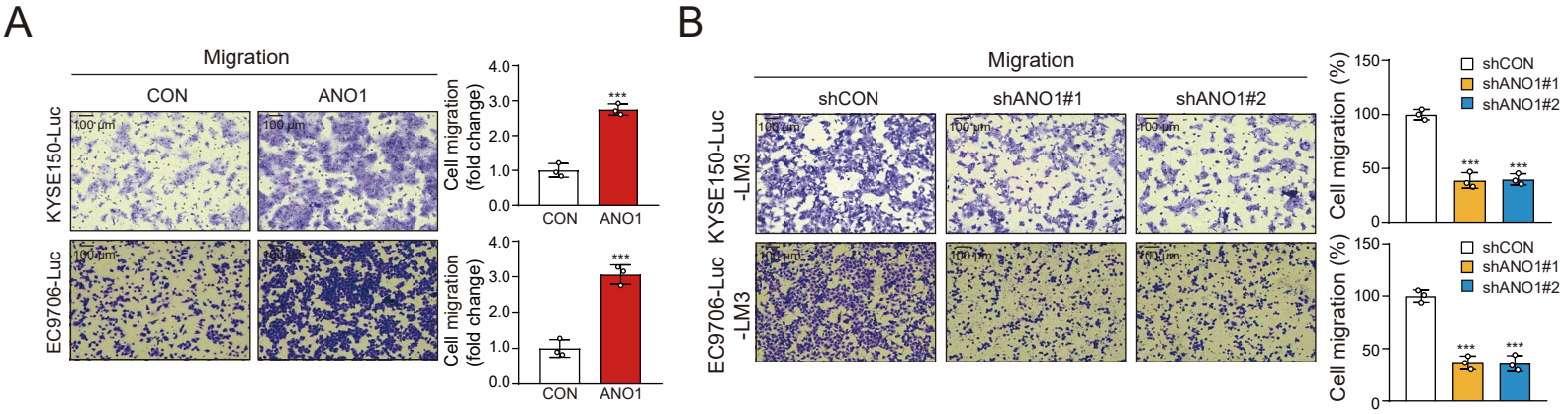

Supplementary Figure 2. (A-B) The migratory capacities of ANO1-overexpressing **(A)** or -knockdown **(B)** ESCC cells was examined by Boyden chamber assay. Bars, SD; ***, $P < 0.001$.

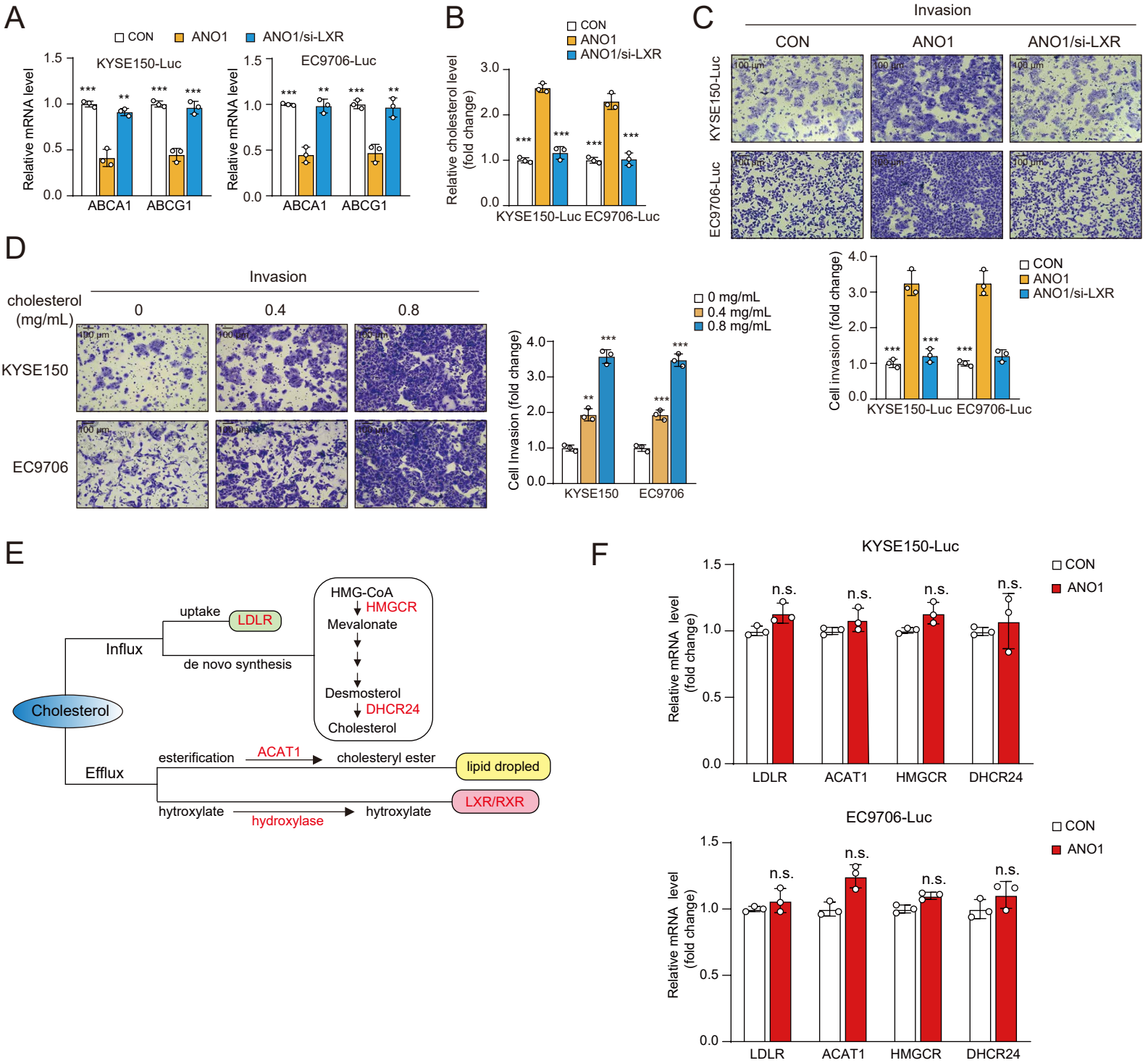

Supplementary Figure 3. (A-C) Analyses of ABCA1 and ABCG1 mRNA levels **(A)**, the intracellular cholesterol levels **(B)**, and the invasive abilities **(C)** in ANO1-overexpressing ESCC cells with or without transfection of the siRNA against LXR. **(D)** The invasive ability of ESCC cells treated with increasing concentrations of cholesterol was examined by Boyden chamber invasion assay. **(E)** Diagram showing the key regulators involved in cholesterol influx and efflux. **(F)** The mRNA levels of LDLR, HMGCR, DHCR24, ACAT1 were detected in ANO1-overexprssing ESCC cells by qRT-PCR. Bars, SD; **, $P < 0.01$; ***, $P < 0.001$; n.s.; no significance.

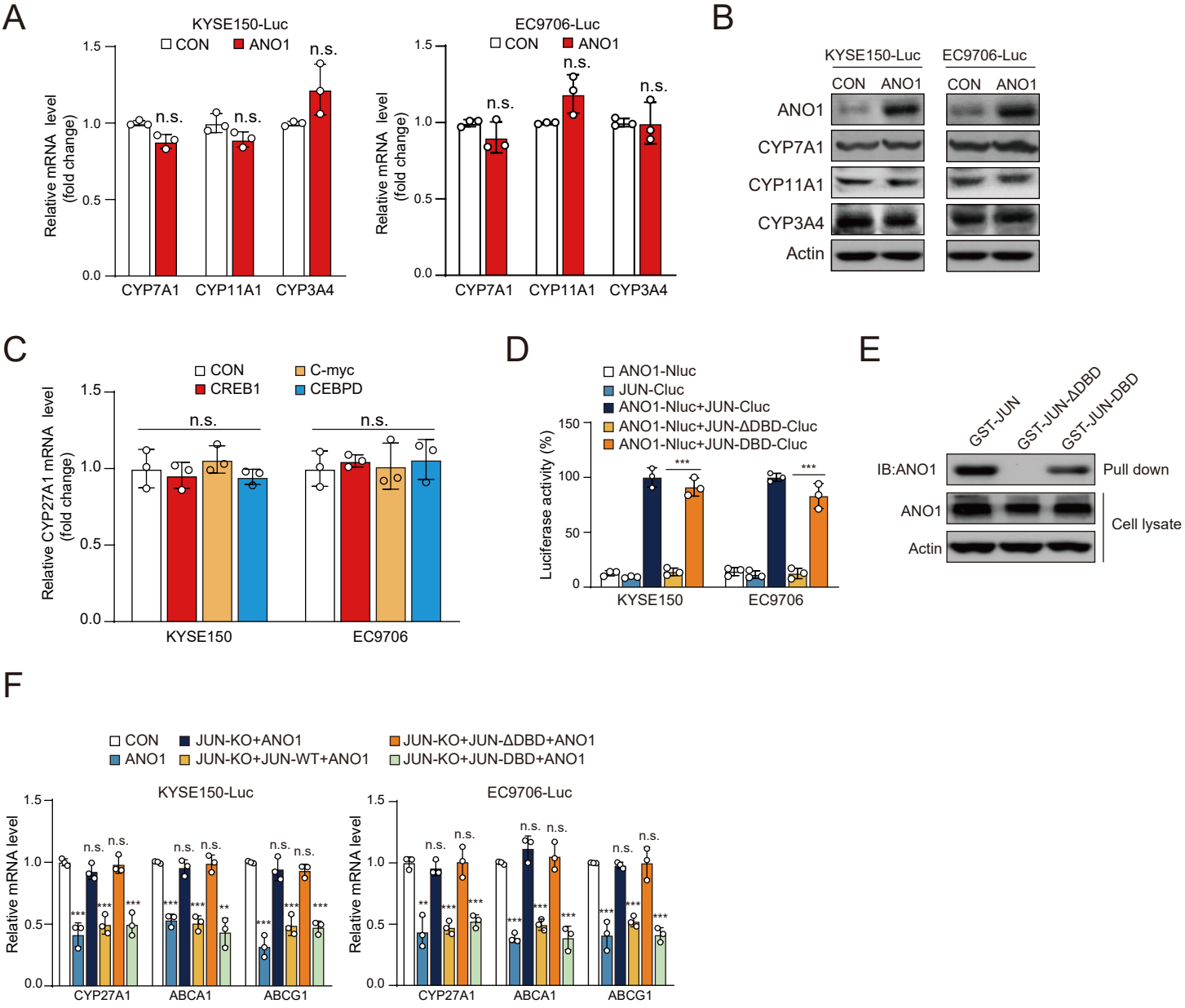

Supplementary Figure 4. (A) qRT-PCR analysis of the mRNA levels of cholesterol hydroxylases CYP7A1, CYP11A1 and CYP3A4 in ANO1-overexpressing ESCC cells. **(B)** Western blot analysis of the protein expression of CYP7A1, CYP11A1 and CYP3A4 in ANO1-overexpressing ESCC and control cells. **(C)** Comparison of CYP27A1 mRNA in ESCC cells transfected with the plasmids overexpressing CREB1, C-myc or CEBPD. **(D)** Luciferase complementation assay revealing the binding of ANO1 with wild-type or different mutants of JUN. **(E)** The interaction between ANO1 wild-type or different mutants of JUN was examined by GST pulldown assay. **(F)** Relative mRNA expression of CYP27A1, ABCA1 and ABCG1 in ESCC cells as indicated was examined by qRT-PCR assay. Bars, SD; **, $P < 0.01$; ***, $P < 0.001$; no significance.

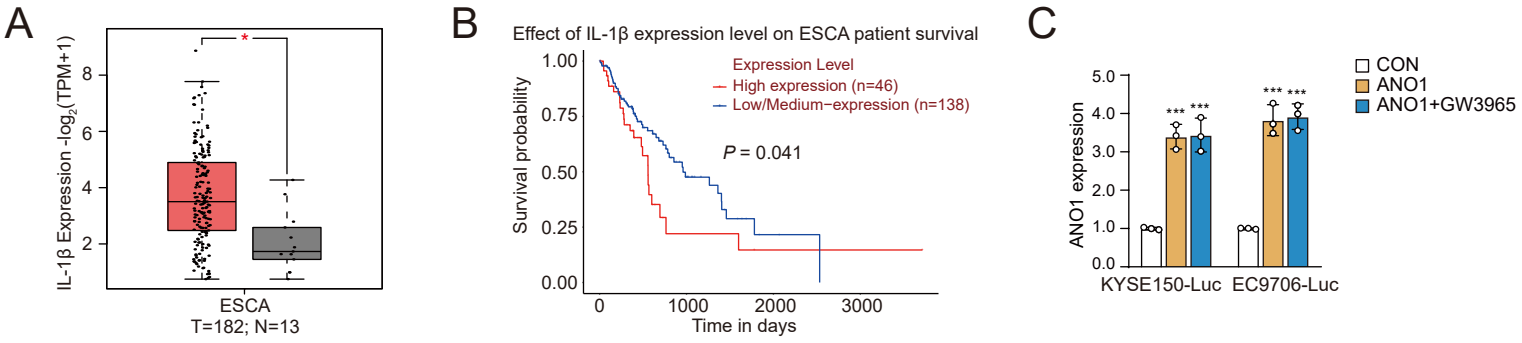

Supplementary Figure 5. (A) The box plots depicting the expression level of IL-1β in the cohort of esophageal carcinoma (ESCA) in the TCGA database. **(B)** Kaplan-Meier analysis of the survival of ESCA patients based on the expression of IL-1β in TCGA database. **(C)** qRT-PCR analyses of ANO1 mRNA level in ANO1-overexpressing ESCC cells with or without GW3965 treatment. Bars, SD; *, $P < 0.05$; ***, $P < 0.001$.

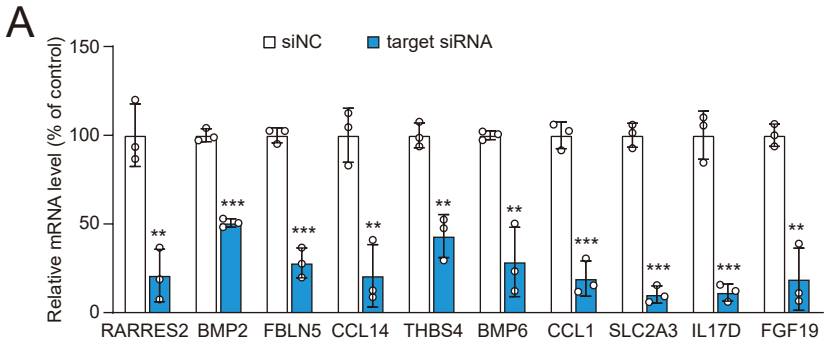

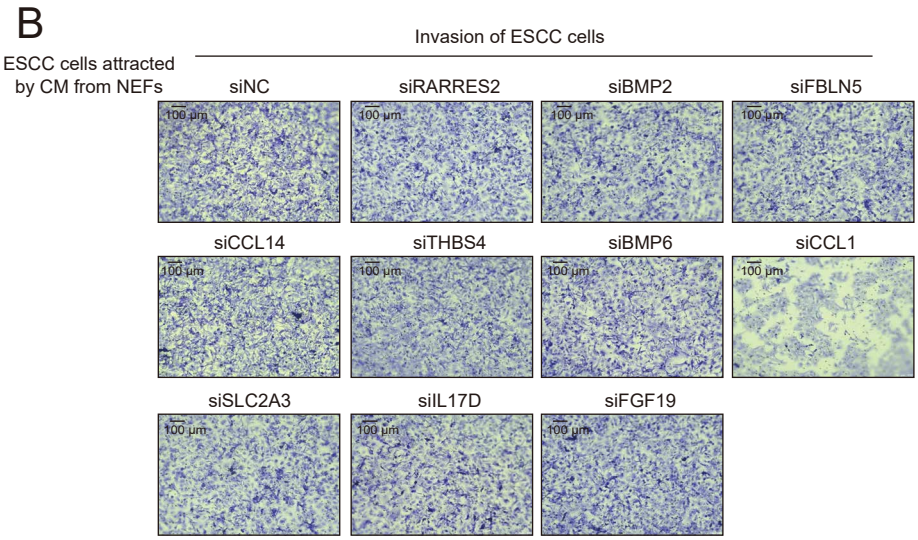

Supplementary Figure 6. (A) Successful knockdown of the 10 candidate genes by siRNAs indicated by qRT-PCR. **(B)** Invasion assay of KYSE150 cells attracted by the supernatant from the fibroblasts transfected with the indicated siRNAs and treated with rIL-1β (20 ng/mL). Bars, SD; **, $P < 0.01$; ***, $P < 0.001$.

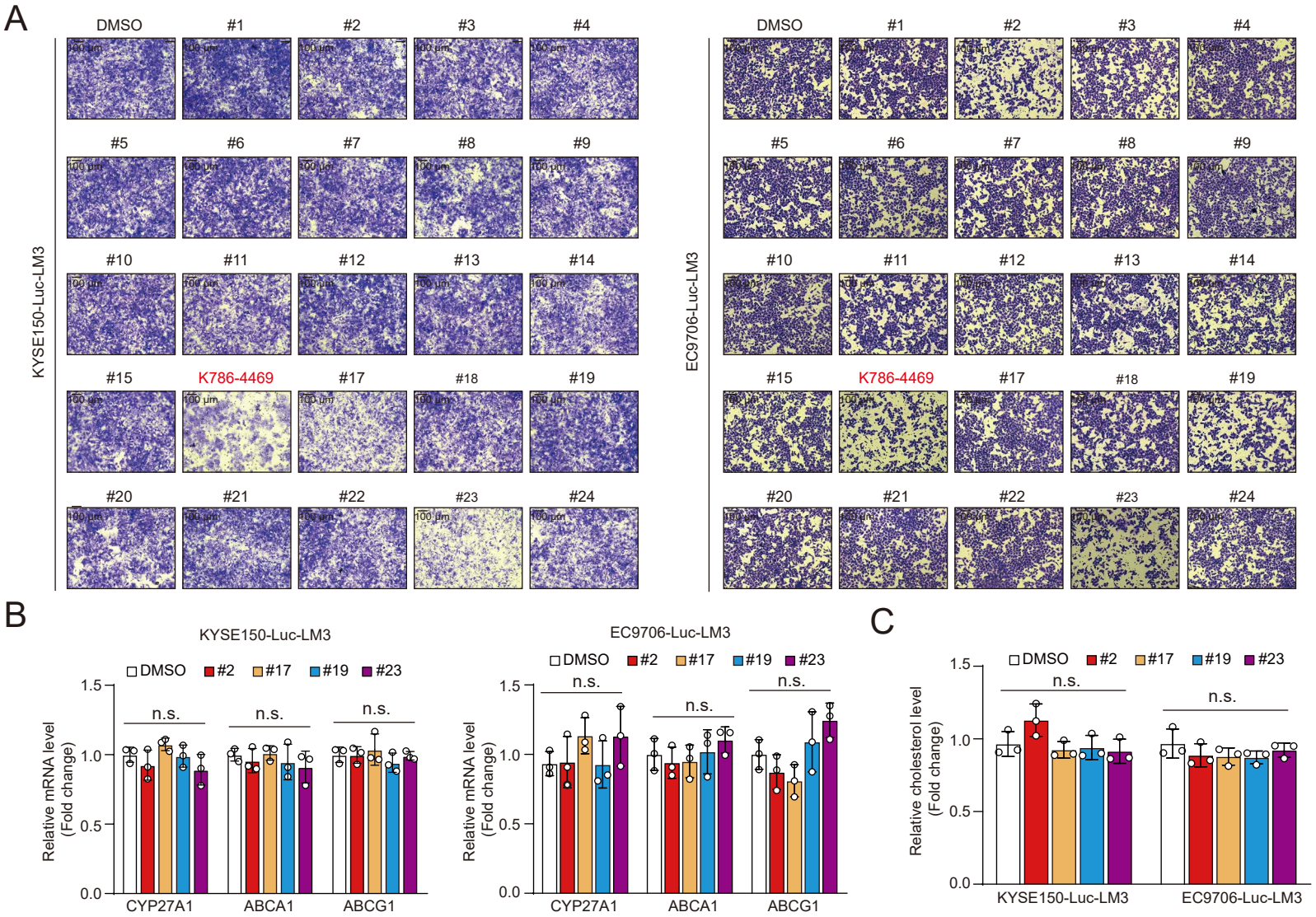

Supplementary Figure 7. (A) Boyden chamber assay was performed to compare the suppressive effects of the 24 candidate compounds on ESCC cell invasion. **(B-C)** Analysis of CYP27A1, ABCA1, ABCG1 expression **(B)** and intracellular cholesterol level **(C)** in ESCC cells treated with the indicated candidate compounds. Bars, SD; n.s.; no significance.

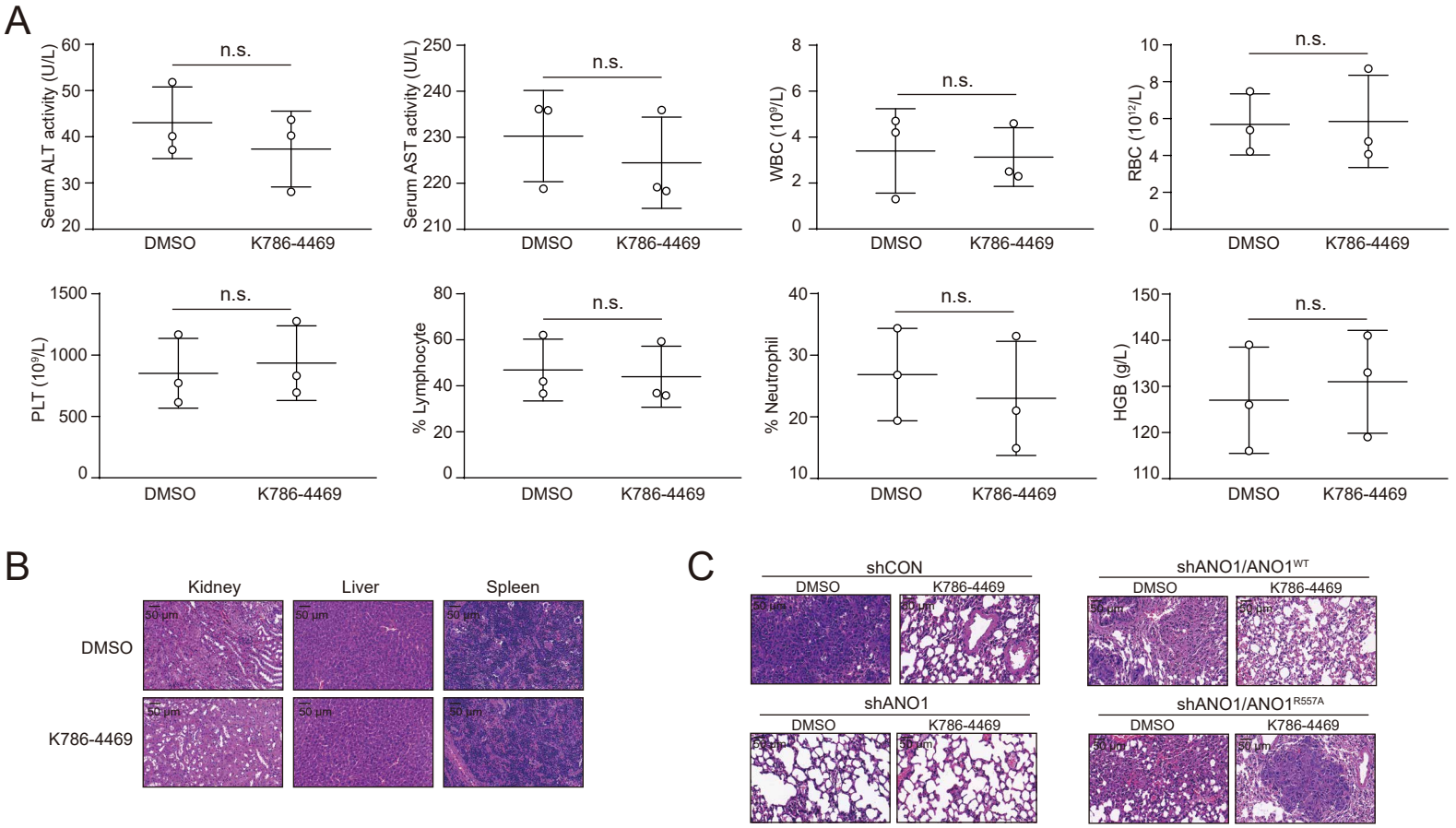

Supplementary Figure 8. (A) Comparison of serum ALT and AST levels, and white blood cells (WBC), red blood cells (RBC), hemoglobin (HGB), platelets (PLT), neutrophils and lymphocytes in mice with or without K786-4469 treatment. **(B)** H&E staining of kidney, liver and spleen of the mice treated with or without K786-4469. **(C)** H&E staining of lung sections as indicated**.** Bars, SD; n.s.; no significance.